International Journal of Mass Spectrometry 280 (2009) 65–71

Contents lists available at ScienceDirect

International Journal of Mass Spectrometry

journal homepage: www.elsevier.com/locate/ijms

Absolute partial cross sections and kinetic energy analysis for the electron impact ionization of ethylene

N. Endstrasser[a], F. Zappa[a], A. Mauracher[a], A. Bacher[a], S. Feil[b], D.K. Bohme[c], P. Scheier[a], M. Probst[a], T.D. Märk[a,d,*]

[a] Institut für Ionenphysik und Angewandte Physik, Universität Innsbruck, Technikerstraße 25 b, 6020 Innsbruck, Austria
[b] Institut de Physique Nucléaire de Lyon, Université Claude Bernard, 43 boulevard du 11 Novembre 1918, 69622 Villeurbanne CEDEX, France
[c] Department of Chemistry, York University, 4700 Keele Street, Toronto, ON, Canada M3J 1P3
[d] Department of Experimental Physics, Comenius University, SK-84248 Bratislava, Slovak Republic

ARTICLE INFO

Article history:
Received 23 May 2008
Received in revised form 6 August 2008
Accepted 7 August 2008
Available online 19 August 2008

Keywords:
Partial cross section
Ethylene
Electron impact ionization
Kinetic energy release
Mass spectrometry

ABSTRACT

We present absolute partial electron impact ionization cross sections for ethylene in the electron energy range between threshold and 1000 eV measured with a two sector field double focusing mass spectrometer. Ion kinetic energy distribution functions have been measured at all electron energies by applying a deflection field method. Multiplication of the measured relative cross sections by the appropriately determined discrimination factors lead to accurate relative partial cross sections. Normalization of the sum of the relative partial cross sections to an absolute total cross section gives absolute partial cross section values. The initial kinetic energy distributions of several fragment ions show the presence of two or more contributions that exhibit different electron energy dependencies. Differential cross sections with respect to the initial kinetic energy of the ions are provided and are related to specific ion production channels. The electron threshold energies for the direct and numerous other dissociative ionization channels are determined by quantum chemical calculation and these allow the determination of the total kinetic energy release and the electron energy loss for the most prominent dissociative ionization channels.

1. Introduction

Cross sections for electron impact ionization of small hydrocarbons such as CH_y, C_2H_y and C_3H_y are required for understanding the physics and chemistry of planetary atmospheres and plasma processing [1–4]. But also the investigation of the influence of hydrocarbon impurities on the plasma burning in fusion experiments needs a deep understanding of the ionization processes, including information about the energy and momentum of reactants and reaction products. Small hydrocarbon species like ethylene are formed by the interaction of the plasma with the surface of carbon fibre composite tiles coating the walls of a plasma vessel. Kinetic Monte Carlo codes are used for the modelling of the transport of impurities within the vessel and these require a detailed knowledge about the inelastic collision processes of electrons with small hydrocarbon species [5,6].

Ethylene (C_2H_4) is the simplest member of the olefinic hydrocarbon series and one of the most important raw materials for the organic chemical industry. It is used in the food industry for accelerating the ripening of bananas, for maturing the colour of citrus fruits and increasing the growth rate of seedlings, vegetables, and fruit trees. The oxyethylene welding and cutting of metals can be mentioned as another common application.

Fragment ions that are formed with high kinetic energies are often collected with considerably reduced efficiency. Poll et al. [7] have demonstrated that ion trajectory calculations for the extraction region of our Nier-type ion source allow the determination of the extraction efficiency at one particular initial kinetic energy. This so-called discrimination factor is used to correct the value of the measured partial ionization cross section at one electron energy.

Although the same fragment ion can be formed in different dissociative ionization processes with different probabilities at a particular electron energy, the ion kinetic energy distribution function exhibits a characteristic shape for each electron energy. The initial kinetic energy of a detected ion that is deflected into the direction perpendicular to the focal plane of the mass spectrometer is proportional to the square of the deflection voltage in that direction. Therefore the kinetic energy distribution can be easily determined by measuring the ion intensity as a function of the deflection potential. Also, the total discrimination factor for the integrated ion yield at one electron energy can be calculated as

* Corresponding author.
E-mail address: Tilmann.Maerk@uibk.ac.at (T.D. Märk).

1387-3806/$ – see front matter © 2008 Elsevier B.V. All rights reserved.
doi:10.1016/j.ijms.2008.08.004

the sum of discrimination factors weighted by the kinetic energy distribution function.

The absolute calibration of relative partial cross sections is realized by normalizing the sum of corrected relative partial cross sections to the sum of the corresponding absolute partial cross sections reported by Tian and Vidal [8]. The normalization factors for the total ionization cross sections are found to be independent of electron energy within limits of experimental error.

2. Experimental

The apparatus used in this study is a double focusing two sector field mass spectrometer of reversed geometry with a Nier-type electron impact ion source and has been described in detail in earlier publications [7,9]. A stagnant target gas is crossed by a well-characterized magnetically collimated electron beam with a FWHM energy spread of ~0.5 eV. Product ions are extracted from the ion source by a strong homogeneous electric field (3 kV/m) generated with a repeller (located in the back of the ion source) and lenses that are part of the front side of the interaction region of the electron beam and the neutral molecules. They are then accelerated to 3 kV before entering the analyzing part of the mass spectrometer through a narrow entrance slit. The ions then pass two pairs of perpendicular deflection plates that allow the ion beam to be steered in the *y*- and *z*-direction. These deflection plates are used in cross section measurements to sweep the extracted ion beam across the entrance slit [10] and to integrate the detected ion signal. After passing through a magnetic sector field followed by an electric sector field, the ions are detected by a secondary electron multiplier operated in the pulse counting mode. The double focusing mass spectrometer corrects for the angular and spatial spreads of the starting points of the ions and for small variations in the kinetic energy within the deflection plane of the magnetic sector. The only way to compensate a velocity component perpendicular to the plane of the instrument (*z*-direction) is to apply a *z*-deflection voltage on a pair of plates right after the ion source. The ion yield, measured as a function of the *z*-deflection voltage, allows the determination of the kinetic energy distribution for a given fragment ion [7,11–14]. The present electron energy scale is calibrated with the onset of the Kr^+ cross section curve published by Rapp and Englander-Golden [15]. Due to the strong electric extraction field, even light fragment ions with initial kinetic energies up to several eV in the *z*-direction are collected and their kinetic energy distributions are measured leading to a complete data set for the investigated molecule using data analysis techniques described in Ref. [16–18].

3. Results and discussion

A mass spectrum of ethylene gas with a purity of 99.5% ionized by 200 eV electrons is shown in Fig. 1. The pressure is set to 1×10^{-5} Pa and the electron current is 5 μA.

The peak assignments given in Fig. 1 include contributions from isotopomers and possible doubly charged ions. Thus singly charged $^{13}C^+$ ions (about 1%) as well as doubly charged $^{13}CCH^{++}$ ions contribute to the peak at *m*/*z* 13. The contribution of $^{13}CCH^{++}$ to the peak at *m*/*z* 13 can be estimated from the C_2H^{++} signal at *m*/*z* 12.5 to be smaller than 0.1%. The ion yield at *m*/*z* 14 can be attributed to the singly charged fragment ion CH_2^+ and the doubly charged parent ion $C_2H_4^{++}$. The peak at *m*/*z* = 29 with an abundance of about 2.8% of the main isotope of $C_2H_4^+$ is due to the isotopomer $^{13}C^{12}CH_4^+$ and the peak at *m*/*z* = 14.5 (see inset in Fig. 1) can be assigned to the doubly charged isotopomer ion $^{13}CCH_4^{++}$. By comparison of the signal of the doubly and singly charged isotopomer ion at *m*/*z* 14.5

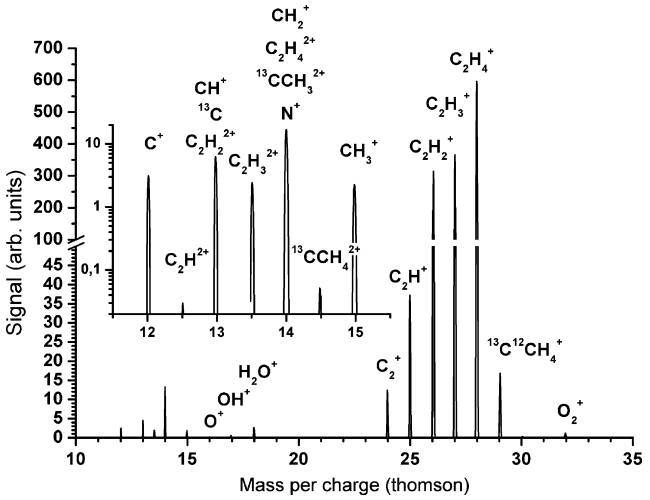

Fig. 1. Mass spectrum of ethylene recorded at an electron energy of 200 eV and an electron current of 5 μA.

and 29, we can estimate the contribution of $^{13}CCH_3^{++}$ to the peak at *m*/*z* 14 to be approximately 10%.

3.1. Absolute partial cross sections

The corrected absolute partial cross sections for individual ions are given in Fig. 2 for *m*/*z* 28–24 on the top, and for *m*/*z* 15–12 in the middle and *m*/*z* 2 and 1 on the bottom (for the contribution of particular ion species to each mass, see the previous paragraph). Absolute cross sections are obtained by normalizing the maximum

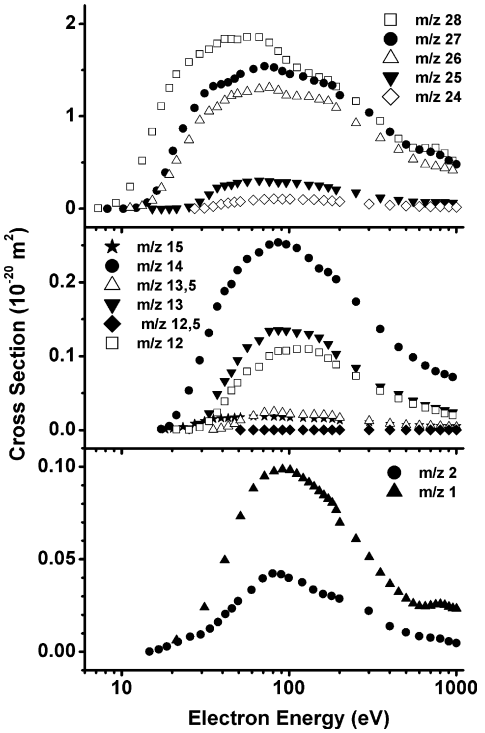

Fig. 2. Absolute partial cross sections for all fragments that are formed by electron impact of ethylene (except for *m*/*z* 1 only every second data point is shown). The sum of the measured relative partial cross sections is normalized to the total cross section of Tian and Vidal [8]. The electron energy scale is calibrated by comparison of our Kr^+ cross section to that of Rapp and Englander-Golden [15].

of the sum of these partial cross sections at the maximum of the corresponding maximum of the absolute total cross sections obtained by Tian and Vidal. Error bars for the partial cross sections before normalization with the data of Ref. [8] are estimated to lie within 15% (taking into account the error in the discrimination factors and in the measured ion currents). Within these error bars there is a good agreement between the present partial cross section data and those of Tian and Vidal except in the case of H^+ for which our cross sections are smaller by a factor of 6.5. This can be explained due to the fact that the stability of the magnet is limited in the region lower than m/z 1.5.

3.2. Ion kinetic energy distributions

For the kinetic energy distribution functions of the fragment ions of ethylene, we make the same observations as in the previous investigations of CH_4 and C_2H_2 [16,17]: in comparison to the quasithermal behavior of the heavier singly and doubly charged C_2H_y ions, the distribution functions of those ions formed out of ethylene by the loss of at least one C atom show contributions of energetic, non-thermal ions (see Figs. 3–5). These graphs are also available in a tabulated form upon request from the corresponding author. The values determined for the mean kinetic energies are presented in Table 1 along with the average kinetic energies of additional contributions. The ions contributing to the kinetic energy spectra are revealed by the careful analysis of the mass spectrum presented in the previous section. We have shown that the major contributions to the ion yields at mass number 12–15, aside from

Table 1
Average kinetic energy values of the different singly and doubly charged fragment ions

Mass number	E_{mean} (meV)	E_{peak1} (meV)	E_{peak2} (meV)	A_{peak1}:A_{peak2}
28	59	–	–	–
27	79	–	–	–
26	93	–	–	–
25	143	–	–	–
24	159	–	–	–
15	502	229	1644	3.97
14	1310	266	2169	0.89
13.5	106	-	-	–
13	984	592	2201	2.52
12.5	242	–	–	–
12	1062	525	2080	1.24
2	1426	102	2489	0.82
1	1516	695	1881	0.48

The average kinetic energy values of the contributions from different ion species composing the measured distribution function are given as $E_{peak\,i}$, and the peaks are numbered in the way that the index 1 stands for the quasithermal contribution (see text).

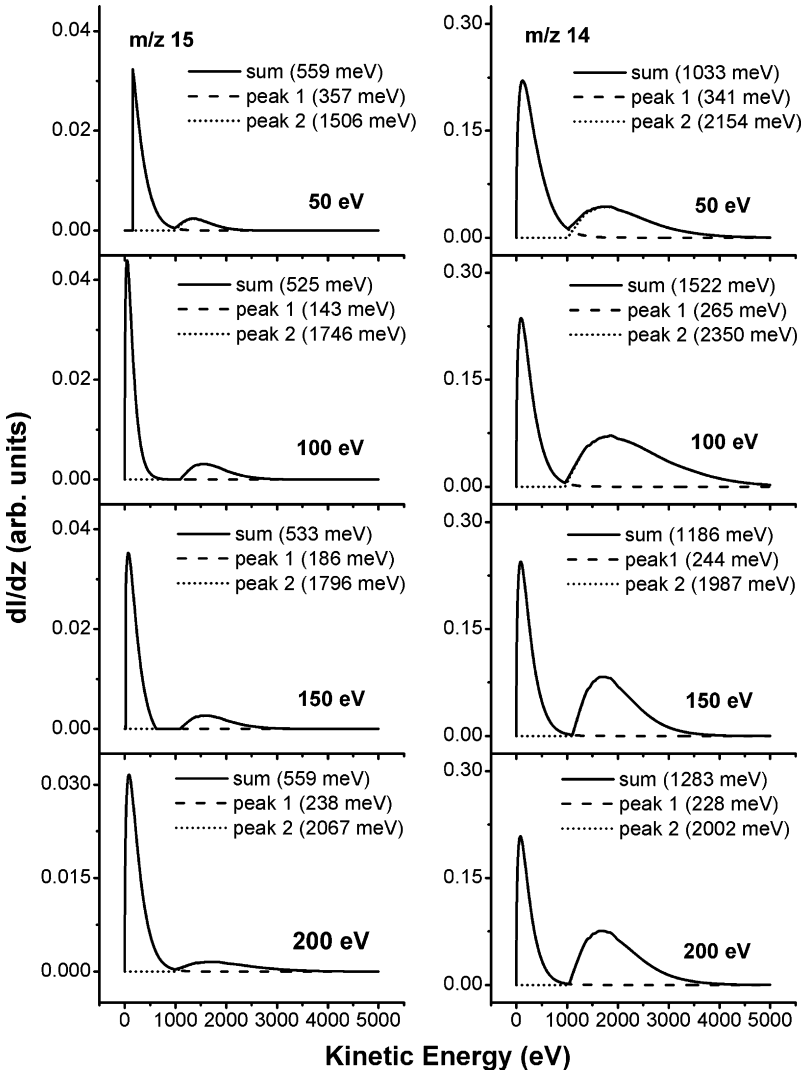

Fig. 3. Ion kinetic energy distributions for CH_3^+ and CH_2^+ ions. The solid line corresponds to the analysis of the z-profiles according to the present method.

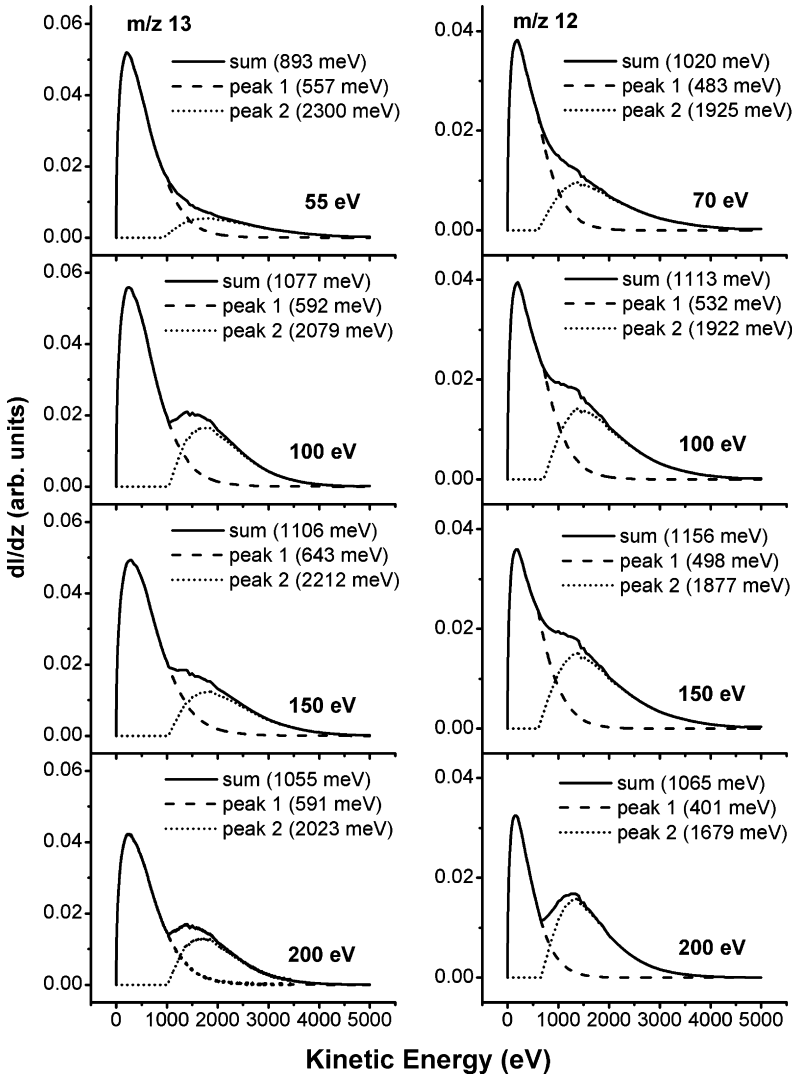

Fig. 4. Ion kinetic energy distributions for CH^+ and C^+ ions. The solid line corresponds to the analysis of the *z*-profiles according to the present method.

the most abundant ethylene fragments CH_y^+ with $0 < y < 3$, are due to: $^{13}CH_2^+$ at *m*/*z* 15, $^{13}CCH_3^{2+}$ at 14, $C_2H_2^{2+}$ at 13 and C_2^{2+} at *m*/*z* 12.

A clear identification of the ion species contributing to the kinetic energy distributions at *m*/*z* 15 can be achieved by cross section curves that are differential with respect to the kinetic energy of the ion (see Fig. 6 giving as an example the cross sections for *m*/*z* 14 and 15). These differential cross sections are deduced from the kinetic energy distributions and the partial cross sections (for details see [16–18]) by separating the energy distribution functions for a certain fragment into a thermal or low energy regime from 0 to 0.5 eV initial kinetic energy (open circles) and a high kinetic energy regime with initial kinetic energies higher than 0.5 eV (open triangles). It is interesting to note that in the two cases shown in Fig. 6 differential cross sections are quite different in magnitude. Whereas for *m*/*z* 15 the cross section for the low energy regime is the dominating one (open circles, upper panel), for *m*/*z* 14 the cross section for the high energy contribution is dominating most likely produced via Coulomb explosion of the doubly charged parent ion (open triangles, lower panel). As a matter of fact taking into account the corresponding isotopic ratio it can be concluded that the high energy contribution for *m*/*z* 15 (open triangles, upper panel) is mainly caused by the isotopomer $^{13}CH_2^+$.

3.3. Total kinetic energy release

Except for the direct ionization, excited states of the reaction products are involved in an inelastic collision event. But information about the excited states is available only for diatomic systems such as CH/CH^+. Therefore several plausible assumptions have to be made in order to allow the calculation of the total kinetic energy E_K released in the dissociative ionization process and to determine the energy loss $E_{el}^{(-)}$ of the impacting electron.

For the determination of the kinetic energy release one needs to take into account, that the molecules of the stagnant gas target already have an initial average kinetic energy $E = 3kT/2$ originating from the thermal energy distribution function

$$W(E) = \text{const}\sqrt{E}\,\exp\left(-\frac{E}{kT}\right).$$

As these molecules are in thermal equilibrium with the surrounding heated walls of the ion source, the velocity distribution function of the molecules is of spherical geometry. Due to the law of momentum conservation the momentum transfer from the incident electron to the parent can be neglected and for the direct ionization, $C_2H_4 + e \rightarrow C_2H_4^+ + 2e$, the spherical geometry of the velocity distribution function is not disturbed. Therefore the ini-

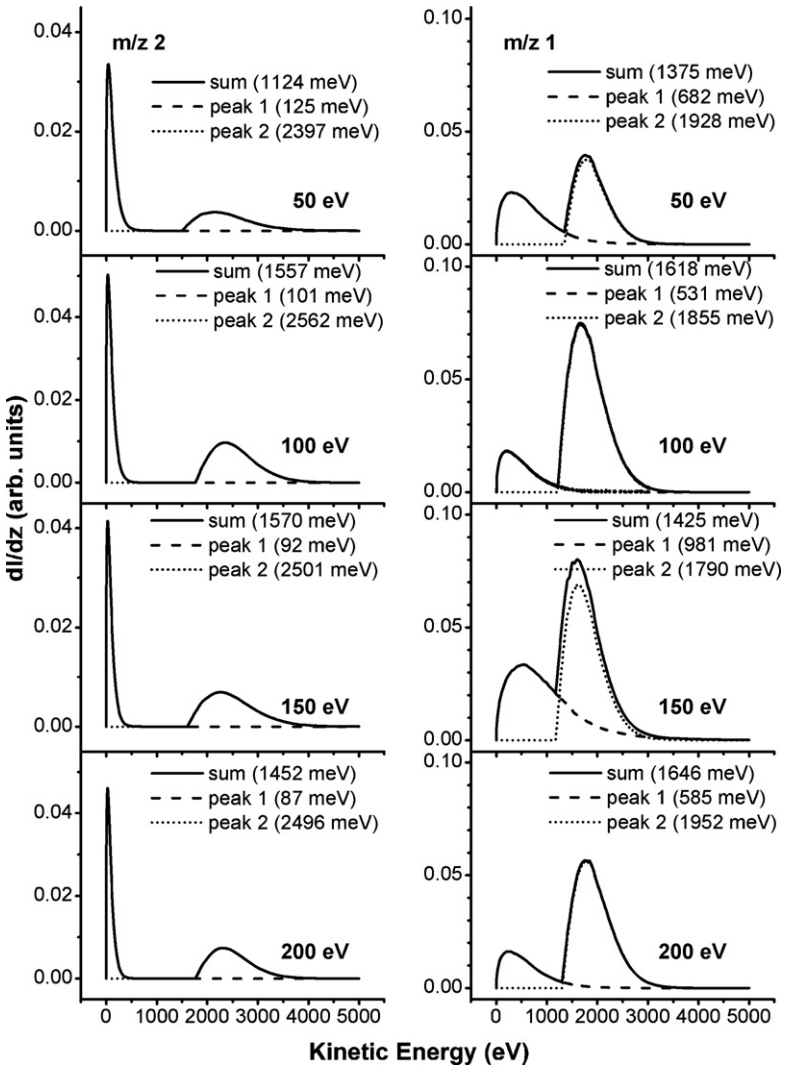

Fig. 5. Ion kinetic energy distributions for H_2^+ and H^+ ions. The solid line corresponds to the analysis of the *z*-profiles according to the present method.

tial kinetic energy is the mean value of the discrimination corrected kinetic energy distribution function measured for $C_2H_4^+$. Due to the random rotation of the molecule in the time between excitation and dissociation, the velocity distribution of the fragment ions are also independent on the direction of the incident electron beam.

While no excited states are involved in the direct ionization process and the energy lost by the incident electron coincides with the ionization potential I_p, the contribution of the direct vibrational dissociation to the total dissociation cross section can be neglected in comparison to the dissociative excitation mechanism. During the dissociative ionization process the incident electron looses an energy of $E_{el}^{(-)}$,

$$E_{el}^{(-)} = I_p(AB) + D_0(AB^+) + \Delta E_{exc}(AB^{+*})$$

where $\Delta E_{exc}(AB^{+*})$ is the excess energy transferred from the incident electron to the parent AB with mass m_0. This energy is released during the dissociation process and constitutes the total kinetic energy E_K of the reaction products A and B with mass m_1 and $m_0 - m_1$. By calculating the reaction threshold energy *E*th corresponding to the sum of the first two terms in the previous equation and measuring the released excess energy ΔE_{exc}, the energy loss of the incident electron can be calculated.

In order to give accurate dissociative ionization threshold values *E*th for each dissociation channel, we have optimized the geometry and have calculated the total energy of all possible fragment molecules at the second-order Møeller-Plesset perturbation (MP2) [19–21] level with the correlation-consistent valence triple-zeta (cc-pVTZ) basis set of Dunning [22] augmented with diffuse functions [23,24]. Due to limit of space in the manuscript we cannot list all detailed results of the calculations. They are available upon request from the corresponding author. The calculated values for each dissociative ionization channel show that the fragmentation of the excited parent into a small number of fragments is energetically favoured. Though we cannot distinguish between the different excited states of the molecules and the excitation cross sections are inversely proportional to the transition energy, we are measuring "average" kinetic energy distributions of the lower excited states of the charged reaction products. Assuming an excitation of the hydrocarbon molecule above the dissociation limit leads rather to a sequential decay into smaller fragments in steps of 2 than splitting into multiple reaction products at once, the total kinetic energy $\overline{E_K}$ released during the dissociation process can be calculated with

$$\overline{E_K} = \frac{\overline{E}_1 \cdot m_0}{m_0 - m_1} - \frac{\overline{E}_0 \cdot m_1}{m_0 - m_1}$$

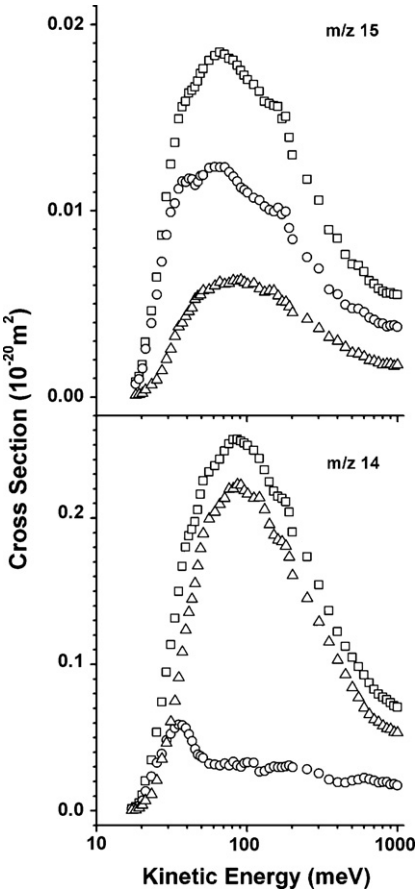

Fig. 6. Absolute partial cross sections (open squares) and absolute differential (with respect to their initial kinetic energy) cross sections corresponding to a low energy quasithermal part (<0.5 eV, open circles) and to a high kinetic energy part (>0.5 eV, open triangles).

where $\overline{E}_0$ and $\overline{E}_1$ are the initial energies of the precursor with mass m_0 and the product ion with mass m_1 [13]. The average kinetic energy of the product ion corresponds to the average quasithermal kinetic energy listed in Table 1 for each fragment ion. While the initial kinetic energy $\overline{E}_0$ of the precursor in the first fragmentation step is the mean value of the measured kinetic energy distribution of $C_2H_4^+$ ions, the average kinetic energy of the fragment ions in a dissociative excited state is higher than those species reaching the detector. Therefore the total kinetic energy released in the second fragmentation step can only be calculated under the assumption that the contribution of the excess energy to the kinetic energy is small enough after the first fragmentation to be neglected. As this assumption for the second fragmentation step is highly speculative, we are only carrying out calculations for the first fragmentation step. We estimate an uncertainty of 30% for the given average kinetic energy values $\overline{E_1}$ of the charged reaction product to each dissociative ionization channel listed in Table 1. As a result the total kinetic energy release values $\overline{E}_K$ presented in Table 2 have an estimated uncertainty ranging from 90% for the C_2– group to 35% for those channels involving the loss of a carbon atom. The uncertainty for the presented values of the mean electron energy loss $\overline{E}_{el}^{(-)}$ lies at 0.5–1 eV (depending on the reaction channel) which is acceptable considering the broad distribution of this value of a few eV. A linear dependence has been observed for the methane family by Djurić et al. [25,26] for D_0 and the excess energy ΔE_{exc}. For ethylene we cannot observe such a linear dependence of the total kinetic energy release and the dissociation energy listed in Table 2.

Table 2
Main electron impact ionization channels for ethylene, their threshold energies, mean total kinetic energies of reaction fragments and mean electron energy losses

Reaction channel	Eth (eV)	$\overline{E}_K$ (eV)	$\overline{E}_{el}^{(-)}$ (eV)
$e + C_2H_4 \rightarrow C_2H_3^+ + H + 2e$	13.78	0.61	14.39
$e + C_2H_4 \rightarrow C_2H_2^+ + H_2 + 2e$	15.78	0.53	16.31
$e + C_2H_4 \rightarrow CH_2 = C^+ + H_2 + 2e$	13.56	0.53	14.09
$e + C_2H_4 \rightarrow CH_3^+ + CH + 2e$	17.38	0.43	17.81
$e + C_2H_4 \rightarrow CH_2^+ + CH_2 + 2e$	18.84	0.47	19.31
$e + C_2H_4 \rightarrow CH^+ + CH_3 + 2e$	18.32	1.05	19.37

4. Conclusions

Relative partial ionization cross sections are measured for a wide range of fragment ions of ethylene. Absolute cross sections are obtained by normalizing the maximum of the sum of these partial cross sections at the maximum of the corresponding absolute total cross sections published by Tian and Vidal. The kinetic energy distribution functions that are presented for those fragments that are formed by the loss of at least one carbon atom show contributions from a quasithermal and a non-thermal, higher energetic component. The average kinetic energy values for each contributing distribution function are given and assigned to the corresponding fragment ion. This allows the determination of the total kinetic energy release and the electron energy loss for the most prominent dissociative ionization channels. These are the first measurements that present a detailed kinetic energy analysis for ethylene that has not been considered in the past. We conclude that the cross section values of the fragment ions determined here have a much higher accuracy than those reported previously.

Acknowledgements

It is a great pleasure to dedicate this article to Prof. Zdenek Herman, honorary professor of the University Innsbruck. We have enjoyed very much to collaborate with him since 20 years and hope to successfully contribute with him on the scientific field of ion-molecule and ion-surface collisions also in the future. The present work is partly supported by the FWF, Wien, and the European Commission, Brussels network program, and has been performed within the Association EURATOM-ÖAW. This work, supported by the European Communities under the contract of Association between EURATOM and the Austrian Academy of Sciences, is carried out within the framework of the European Fusion Development Agreement. The views and opinions expressed herein do not necessarily reflect those of the European Commission. One of the authors T.D.M. is an adjunct professor at Department of Experimental Physics, University, SK-84248 Bratislava, Slovak Republic.

References

[1] R.K. Janev (Ed.), Atomic and Molecular Processes in Fusion Edge Plasmas, Plenum, New York, 1995.
[2] M.C. McMaster, W.L. Hsu, M.E. Coltrin, D.S. Dandy, C. Fox, Diamond Relat. Mater. 4 (1995) 1000.
[3] H.W. Moos, J.T. Clark, Astrophys. J. 229 (1979) L107.
[4] T.C. Owen, J. Caldwel, A.R. Rivolo, V. Moore, A.L. Lane, C. Sagan, H. Hunt, C. Ponnamperuma, Astrophys. J. 236 (1987) L39.
[5] R.K. Janev, D. Reiter, Phys. Plasmas 9 (2002) 4071.
[6] R.K. Janev, D. Reiter, Phys. Plasmas 11 (2004) 780.
[7] H.U. Poll, V. Grill, S. Matt, N. Abramzon, K. Becker, P. Scheier, T.D. Märk, Int. J. Mass Spectrom. Ion Proc. 177 (1998) 143.
[8] C. Tian, C.R. Vidal, Chem. Phys. Lett. 288 (1998) 499.
[9] V. Grill, G. Walder, D. Margreiter, T. Rauth, H.U. Poll, P. Scheier, T.D. Märk, Z. Phys. D 25 (1993) 217.
[10] V. Grill, G. Walder, P. Scheier, M. Kurdel, T.D. Märk, Int. J. Mass Spectrom. Ion Proc. 129 (1993) 31.
[11] R. Taubert, Z. Naturforschg. 19a (1964) 484.
[12] R. Fuchs, R. Taubert, Z. Naturforschg. 19a (1964) 494.

[13] R. Taubert, Z. Naturforschg. 19a (1964) 911.
[14] R. Fuchs, R. Taubert, Z. Naturforschg. 19a (1964) 1181.
[15] D. Rapp, P. Englander-Golden, J. Chem. Phys. 43 (1965) 1464.
[16] K. Gluch, P. Scheier, W. Schustereder, T. Tepnual, L. Feketeova, C. Mair, S. Matt-Leubner, A. Stamatovic, T.D. Märk, Int. J. Mass Spectrom. 228 (2003) 307.
[17] S. Feil, A. Bacher, M. Zangerl, W. Schustereder, K. Gluch, P. Scheier, Int. J. Mass Spectrom. 233 (2004) 325.
[18] S. Feil, K. Gluch, A. Bacher, S. Matt-Leubner, D.K. Böhme, P. Scheier, T.D. Märk, J. Chem. Phys. 124 (2006) 1.
[19] P.H. Dawson, T.W. Tickner, J. Chem. Phys. 37 (1962) 672.
[20] K. Buchheit, W. Henkes, Z. Angew. Phys. 24 (1968) 191.
[21] R. Clampit, L. Gowland, Nature (London) 223 (1969) 816.
[22] T.H. Dunning, J. Chem. Phys. 90 (1989) 1007.
[23] D.E. Woon, T.H. Dunning, J. Chem. Phys. 98 (1993) 1358.
[24] R.A. Kendall, T.H. Dunning, R.J. Harrison, J. Chem. Phys. 96 (1992) 6796.
[25] N. Djurić, Y.S. Chung, B. Walbank, G.H. Dunn, Phys. Rev. A 58 (1997) 2887.
[26] N. Djurić, S. Zhou, G.H. Dunn, M.E. Bannister, Phys. Rev. A 68 (1998) 304.